

OMTN, Volume 31

Supplemental information

**Chemically modified small interfering
RNA targeting Hedgehog signaling
pathway for rheumatoid arthritis therapy**

Lang Lin, Shangling Zhu, Hongyu Huang, Lin-Ping Wu, and Jianlin Huang

Table S1. The sequences of naked siRNA targeting SMO mRNA.

siRNA	Strand	Sequence (5'-3')
si-h-1	S	CUACGUCAAUGCGUGCUUCdTdT
	AS	GAAGCACGCAUUGACGUAGdTdT
si-h-2	S	CGUCA AUGCGUGCUUCUUUdTdT
	AS	AAAGAAGCACGCAUUGACGdTdT
si-h-3	S	CGAGGAGUCAUGACUCUGUdTdT
	AS	ACAGAGUCAUGACUCCUCGdTdT
si-h-4	S	UGACUCUGUUCUCAUCAAdTdT
	AS	UUGAUGGAGAACAGAGUCAAdTdT
si-h-5	S	UCUUUGUCAUCGUGUACUAdTdT
	AS	UAGUACACGAUGACAAAGAdTdT
si-h-6	S	UGCCCAAGUGUGAGAAUGAdTdT
	AS	UCAUUCUCACACUUGGGCAdTdT
si-h-7	S	UCGCUACCCUGCUGUUUUdTdT
	AS	AAUAACAGCAGGGUAGCGAdTdT
si-h-8	S	GCCACUUCUACGACUUCUUdTdT
	AS	AAGAAGUCGUAGAAGUGGCdTdT
si-h/m-1	S	CAUGCCCAAGUGUGAGAAUdTdT
	AS	AUUCUCACACUUGGGCAUGdTdT
si-h/m-2	S	AGGACAUGCACAGCUACAAdTdT
	AS	AUGUAGCUGUGCAUGUCCUdTdT
si-h/m-3	S	UGGGAGGCUACUCCUCAUdTdT
	AS	AUGAGGAAGUAGCCUCCAdTdT
si-h/m-4	S	GCCUGGGCAUUUUUGGCUUdTdT
	AS	AAGCCAAAAAUGCCCAGGCdTdT
si-NC	S	UUCUCCGAACGUGUCACGUdTdT
	AS	ACGUGACACGUUCGGAGAAAdTdT

Abbreviations: siRNA, small interfering RNA; SMO, Smoothened; mRNA, messenger RNA; NC, negative control; S, sense strand; AS, antisense strand; A, adenine; U, uracil; G, guanine; C, cytosine; dT, deoxy thymine.

Table S2. The sequences of chemically modified siRNA.

siRNA	Strand	Sequence (5'-3')
si-S1A1	S	mAmGmGACAUGCACAGCUAmCmAmUdTdT
	AS	phos-mAmUmGUAGCUGUGCAUGUmCmCmUdTdT
si-S1A2	S	mAmGmGACAUGCACAGCUAmCmAmUdTdT
	AS	phos-mAmUmGUAGCUmGfUmGCAUGUmCmCmUdTdT
si-S1A3	S	mAmGmGACAUGCACAGCUAmCmAmUdTdT
	AS	phos-mAmUmGUAmGfCfUmGfUmGCmAUmGUmCmCmUdTdT
si-S1A4	S	mAmGmGACAUGCACAGCUAmCmAmUdTdT
	AS	phos-mAmUmGfUmAmGfCfUmGfUmGfCmAfUmGfUmCmCmUdTdT
si-S2A1	S	mAmGmGACAUGfCmAfCAGCUAmCmAmUdTdT
	AS	phos-mAmUmGUAGCUGUGCAUGUmCmCmUdTdT
si-S2A2	S	mAmGmGACAUGfCmAfCAGCUAmCmAmUdTdT
	AS	phos-mAmUmGUAGCUmGfUmGCAUGUmCmCmUdTdT
si-S2A3	S	mAmGmGACAUGfCmAfCAGCUAmCmAmUdTdT
	AS	phos-mAmUmGUAmGfCfUmGfUmGCmAUmGUmCmCmUdTdT
si-S2A4	S	mAmGmGACAUGfCmAfCAGCUAmCmAmUdTdT
	AS	phos-mAmUmGfUmAmGfCfUmGfUmGfCmAfUmGfUmCmCmUdTdT
si-S3A1	S	mAmGmGAfCAfUGfCmAfCmAmGfCUAmCmAmUdTdT
	AS	phos-mAmUmGUAGCUGUGCAUGUmCmCmUdTdT
si-S3A2	S	mAmGmGAfCAfUGfCmAfCmAmGfCUAmCmAmUdTdT
	AS	phos-mAmUmGUAGCUmGfUmGCAUGUmCmCmUdTdT
si-S3A3	S	mAmGmGAfCAfUGfCmAfCmAmGfCUAmCmAmUdTdT
	AS	phos-mAmUmGUAmGfCfUmGfUmGCmAUmGUmCmCmUdTdT
si-S3A4	S	mAmGmGAfCAfUGfCmAfCmAmGfCUAmCmAmUdTdT
	AS	phos-mAmUmGfUmAmGfCfUmGfUmGfCmAfUmGfUmCmCmUdTdT
si-S4A1	S	mAmGmGmAfCmAfUmGfCmAfCmAmGfCfUmAmCmAmUdTdT
	AS	phos-mAmUmGUAGCUGUGCAUGUmCmCmUdTdT
si-S4A2	S	mAmGmGmAfCmAfUmGfCmAfCmAmGfCfUmAmCmAmUdTdT
	AS	phos-mAmUmGUAGCUmGfUmGCAUGUmCmCmUdTdT
si-S4A3	S	mAmGmGmAfCmAfUmGfCmAfCmAmGfCfUmAmCmAmUdTdT
	AS	phos-mAmUmGUAmGfCfUmGfUmGCmAUmGUmCmCmUdTdT
si-S4A4	S	mAmGmGmAfCmAfUmGfCmAfCmAmGfCfUmAmCmAmUdTdT
	AS	phos-mAmUmGfUmAmGfCfUmGfUmGfCmAfUmGfUmCmCmUdTdT

Abbreviations: siRNA, small interfering RNA; S, sense strand; AS, antisense strand; A, adenine; U, uracil; G, guanine; C, cytosine; dT, deoxy thymine; m, 2'-O-methyl; f, 2'-Fluoro; phos-, 5'-Phosphate.

Table S3. The sequences of chemically modified siRNA conjugated with cholesterol.

siRNA	Strand	Sequence (5'-3')
si-S1A3-Chol	S	mAmGmGACAUGCACAGCUAmCmAmUdTdT-Chol
	AS	phos-mAmUmGUAmGfCfUmGfUmGCmAUmGUmCmCmUdTdT
si-S1A4-Chol	S	mAmGmGACAUGCACAGCUAmCmAmUdTdT-Chol
	AS	phos-mAmUmGfUmAmGfCfUmGfUmGfCmAfUmGfUmCmCmUdTdT
si-Scr-Chol	S	mUmAmCAUCGACACGUACAmGmGmAdTdT-Chol
	AS	phos-mUmCmCUGmUfAfCmGfUmGUmCGmAUmGmUmAdTdT

Abbreviations: siRNA, small interfering RNA; S, sense strand; AS, antisense strand; Scr, scrambled siRNA; A, adenine; U, uracil; G, guanine; C, cytosine; dT, deoxy thymine; m, 2'-O-methyl; f, 2'-Fluoro; phos-, 5'-Phosphate; -Chol, 3'-Cholesterol.

Table S4. The expression of top 100 similar transcripts.

Number	Gene symbol	Accession	No. of matches	log ₂ FoldChange	P value	adjusted P value
1	SMO	NM_005631.5	19	-1.581578228	4.71E-28	4.32E-26
2	<i>GRIN2D</i>	NM_000836.4	17	-0.337664881	0.364320202	0.565037153
3	<i>GRIA2</i>	NM_001083619.3	15	1.653186782	0.547566006	1
4	<i>UGGT1</i>	NM_020120.4	14	-0.081736214	0.248417371	0.437435049
5	<i>WDFY4</i>	NM_001394531.1	14	-0.527920958	0.77526486	1
6	UBE2G1	NM_003342.5	14	-1.233954249	1.68E-30	1.8E-28
7	<i>PCLO</i>	NM_033026.6	13	1.596328256	0.596458807	1
8	<i>MOB3B</i>	NM_024761.5	13	-2.031495538	0.245266661	1
9	<i>NDUFAF6</i>	NM_152416.4	13	0.19535221	0.281633821	0.476792989
10	<i>NUDT21</i>	NM_007006.3	13	-0.362331723	0.000740126	0.004156914
11	<i>HUWE1</i>	NM_031407.7	13	0.029165164	0.733056968	0.856240949
12	<i>PIGS</i>	NM_033198.4	13	-0.313745649	0.000243344	0.001556904
13	<i>PLEKHA2</i>	NM_021623.2	13	0.539724833	0.0000238	0.00019514
14	<i>GRK6</i>	NM_001004106.3	13	0.057073887	0.629127014	0.787626826
15	<i>TMEM266</i>	NM_152335.3	13	-0.478179458	0.33263856	0.533079197
16	<i>FBXO36</i>	NM_174899.5	13	-0.019803818	0.940999004	0.970361153
17	<i>OTUD7A</i>	NM_001382637.1	13	0.249975011	0.813253682	1
18	<i>RFFL</i>	NM_001017368.2	13	0.423830891	0.00588671	0.024457785
19	<i>SLC26A5</i>	NM_198999.3	13	ND	ND	ND
20	<i>KBTBD7</i>	NM_032138.7	13	-0.914605949	0.0000134	0.000116335
21	<i>ENTPD6</i>	NM_001247.5	13	-0.03950115	0.650585546	0.802077041
22	<i>INKA1</i>	NM_203370.2	13	0.119451686	0.621958318	0.782696773
23	<i>TRIB3</i>	NM_021158.5	13	-0.139729939	0.053455602	0.145699231
24	<i>PAX1</i>	NM_001257096.2	13	-1.854264571	0.086947923	1
25	<i>ACTR5</i>	NM_024855.4	12	0.020331516	0.835582489	0.918039459
26	<i>SHISAL2A</i>	NM_001042693.3	12	ND	ND	ND
27	<i>TPD52L1</i>	NM_003287.4	12	-0.196756897	0.02424368	0.078446261
28	<i>EDEM1</i>	NM_014674.3	12	0.280014938	0.001119633	0.005955408
29	<i>CD276</i>	NM_001024736.2	12	-0.124490963	0.041773671	0.120181868
30	<i>SHISAL2B</i>	NM_001164442.2	12	2.641930609	0.407897946	1
31	<i>BMP1</i>	NM_006129.5	12	0.031500623	0.686169287	0.825591286
32	PLXNC1	NM_005761.3	12	-1.456652731	0.000808984	0.004487005
33	<i>COMMD8</i>	NM_017845.5	12	0.192966542	0.15346262	0.315554339
34	<i>HERC1</i>	NM_003922.4	12	0.163195221	0.124550761	0.271919425
35	<i>TMEM9B</i>	NM_020644.3	12	-0.349271642	0.000203291	0.00133031
36	<i>NPAS2</i>	NM_002518.4	12	-0.549699535	0.00000422	0.0000404
37	<i>STK32C</i>	NM_173575.4	12	-0.042943503	0.781519114	0.886442541
38	<i>SPAG9</i>	NM_001130528.3	12	0.341465239	0.0000131	0.000113954
39	<i>CCDC71</i>	NM_022903.4	12	-0.169468693	0.193680428	0.370808673
40	CCN4	NM_003882.4	12	-1.172069865	6.08E-35	8.89E-33
41	<i>NUDT3</i>	NM_006703.4	12	0.209764731	0.224923759	0.409201619
42	<i>PAPPA</i>	NM_002581.5	12	-0.158702353	0.236588574	0.423808563
43	<i>CNOT1</i>	NM_016284.5	12	0.008390124	0.928283521	0.963946975
44	<i>PLB1</i>	NM_153021.5	12	-0.054391022	0.911084019	0.956673486
45	<i>IKZF3</i>	NM_012481.5	12	ND	ND	ND
46	<i>KDM4D</i>	NM_018039.3	12	-0.131656502	0.845587886	1
47	<i>TRIOBP</i>	NM_001039141.3	12	0.70236634	8.82E-28	7.96E-26
48	<i>CAPN2</i>	NM_001748.5	12	0.582651226	1.79E-24	1.17E-22
49	<i>CATSPERD</i>	NM_152784.4	12	1.976982283	0.447152159	1
50	<i>PPP1R12A</i>	NM_002480.3	12	-0.292016359	0.001065143	0.00570012

51	<i>TOMM22</i>	NM_020243.5	12	0.595599724	0.00000117	0.0000125
52	<i>RHBDD1</i>	NM_001167608.3	12	-0.044719417	0.679061475	0.820774924
53	<i>SLC25A39</i>	NM_001143780.3	12	0.023570839	0.801141988	0.898724696
54	<i>VAR51</i>	NM_006295.3	12	ND	ND	ND
55	<i>RPUSD4</i>	NM_032795.3	12	-0.22326424	0.08380885	0.203321632
56	<i>DUSP3</i>	NM_004090.4	12	0.32148802	0.000834723	0.004614324
57	<i>PTPRF</i>	NM_002840.5	12	0.381352771	0.0000215	0.000177797
58	<i>SORCS3</i>	NM_014978.3	12	ND	ND	ND
59	<i>XPNPEP3</i>	NM_022098.4	12	-0.962206924	9.51E-12	2.17E-10
60	<i>UTP25</i>	NM_014388.7	12	0.182366767	0.102135193	0.235260099
61	<i>SPIRE2</i>	NM_032451.2	12	-0.079166663	0.713131575	0.84390253
62	<i>FRMD1</i>	NM_024919.6	12	ND	ND	ND
63	<i>UBR2</i>	NM_001363705.2	12	0.280956048	0.003939603	0.017561661
64	<i>FLNB</i>	NM_001457.4	12	0.443591128	0.00000017	0.00000209
65	<i>SORCS2</i>	NM_020777.3	12	-0.124300743	0.292467351	0.489429479
66	<i>SIKE1</i>	NM_025073.3	12	0.051177396	0.602546478	0.767784905
67	<i>FAM227A</i>	NM_001013647.2	12	-0.527534496	0.083663697	0.20313464
68	<i>BICC1</i>	NM_001080512.3	12	-0.640274508	1.13E-17	4.54E-16
69	<i>CDH22</i>	NM_021248.3	12	ND	ND	ND
70	<i>CTRC</i>	NM_007272.3	12	1.967429765	0.287436342	1
71	<i>RTTN</i>	NM_173630.4	12	-0.424187768	0.007033916	0.028325512
72	<i>FLRT2</i>	NM_013231.6	12	-0.098259767	0.228004107	0.413193401
73	<i>PIK3C2A</i>	NM_002645.4	12	-0.608827163	0.000000118	0.00000149
74	<i>TRAPPC2L</i>	NM_001318525.2	12	-0.148992416	0.222500379	0.406477978
75	<i>CYP11B1</i>	NM_000497.4	12	ND	ND	ND
76	<i>RHOXF2</i>	NM_032498.3	12	-1.743646521	0.665729628	1
77	<i>ZBTB11</i>	NM_014415.4	12	-0.144786188	0.218312934	0.400791064
78	<i>UBE2L5</i>	NM_001355247.2	12	-0.723496779	0.819994774	1
79	<i>ACTR5</i>	NM_005735.4	12	0.13426405	0.567321992	0.739704983
80	<i>SF3B1</i>	NM_012433.4	12	-0.08260555	0.227841535	0.413099489
81	HELLS	NM_018063.5	12	-1.722568363	1.52E-16	5.53E-15
82	<i>PIK3C2G</i>	NM_001288772.2	12	ND	ND	ND
83	<i>RAX2</i>	NM_001319074.4	12	ND	ND	ND
84	<i>SERPINA9</i>	NM_175739.4	12	1.17786226	0.443888454	1
85	<i>MMAA</i>	NM_172250.3	12	-0.190040075	0.263013942	0.454478907
86	<i>CASP10</i>	NM_032977.4	12	-0.213849221	0.693835672	0.83052456
87	<i>SH3TC2</i>	NM_024577.4	12	0.40258154	0.335383452	0.536038683
88	<i>CCND1</i>	NM_053056.3	12	0.750302999	4.89E-35	7.22E-33
89	<i>TENM1</i>	NM_001163278.2	12	1.985323203	0.447382052	1
90	<i>TTN</i>	NM_001267550.2	12	0.566895677	0.002445276	0.011678462
91	<i>TDRD1</i>	NM_001395205.1	12	2.150231711	0.589919457	1
92	<i>MACF1</i>	NM_001394062.1	12	0.154639839	0.080470033	0.196983247
93	<i>NTRK3</i>	NM_001012338.3	12	-0.052478469	0.954039881	1
94	<i>TNS1</i>	NM_001387777.1	12	0.01326558	0.882843708	0.943690222
95	<i>PAIP2B</i>	NM_020459.1	12	0.125788922	0.853087671	1
96	<i>COPA</i>	NM_004371.4	11	0.158176758	0.012685144	0.046075281
97	<i>MUC6</i>	NM_005961.3	11	ND	ND	ND
98	<i>LYPLA2</i>	NM_007260.3	11	0.445295574	0.0000689	0.00050934
99	<i>SOX11</i>	NM_003108.4	11	0.040000636	0.948194183	0.974650859
100	<i>PHF3</i>	NM_001370348.2	11	0.192480682	0.075094142	0.1875782

Abbreviations: No. of matches, the number of matched sequences between si-S1A3-Chol and similar transcripts; FoldChange, the fold change of transcripts' reads between si-S1A3-Chol versus blank control; ND, not detected in RNA-seq data.

Table S5. Summary of plasma pharmacokinetic parameters for si-S1A3-Chol in rats following single IV or IA administration.

Pharmacokinetics parameters	sense strand		antisense strand	
	IV	IA	IV	IA
C_{max} (nmol/L)	49.53 ± 25.14	2.81 ± 1.13	31.83 ± 11.24	0.37 ± 0.11
t_{max} (h)	0.08 ± 0.00	0.28 ± 0.12	0.08 ± 0.00	0.42 ± 0.08
AUC (nmol/L*h)	23.58 ± 5.69	3.15 ± 0.62	12.67 ± 3.23	1.94 ± 0.30

Abbreviations: IV, intravenous; IA, intra-articular; SEM, standard error of mean; C_{max} , the maximum measured concentration; t_{max} , the time to reach the maximum measured concentration; AUC, area under the concentration-time profile from time zero to the last time point. Data were presented as mean ± SEM.

Table S6. The primer sequences used for qPCR analysis.

Target gene	Primer	Sequence (5'-3')
<i>GAPDH</i>	Forward	CCCATGGCAAATTCCATGGCACCG
	Reverse	GTCATGGATGACCTTGGCCAGGGG
<i>SMO</i>	Forward	CATCAAGTTCAACAGTTCAGGC
	Reverse	AATAACAGCAGGGTAGCGATTC
<i>Gapdh</i>	Forward	CATCACTGCCACCCAGAAGACTG
	Reverse	ATGCCAGTGAGCTTCCCGTTCAG
<i>Smo</i>	Forward	GAGGCTACTTCCTCATCAGAGG
	Reverse	GCTGAAGGTGATGAGCACAAAGC
si-S1A3-Chol-S	RT	miR8006091 (Ribobio)
	Forward	miR8006092 (Ribobio)
	Reverse	ssD089261711 (Ribobio)
si-S1A3-Chol-AS	RT	miR8006129 (Ribobio)
	Forward	miR8006130 (Ribobio)
	Reverse	ssD089261711 (Ribobio)

Abbreviations: qPCR, quantitative real-time polymerase chain reaction; GAPDH, glyceraldehyde-3-phosphate dehydrogenase; SMO, Smoothened; siRNA, small interfering RNA; S, sense strand; AS, antisense strand; RT, reverse transcription; A, adenine; T, thymine; G, guanine; C, cytosine.

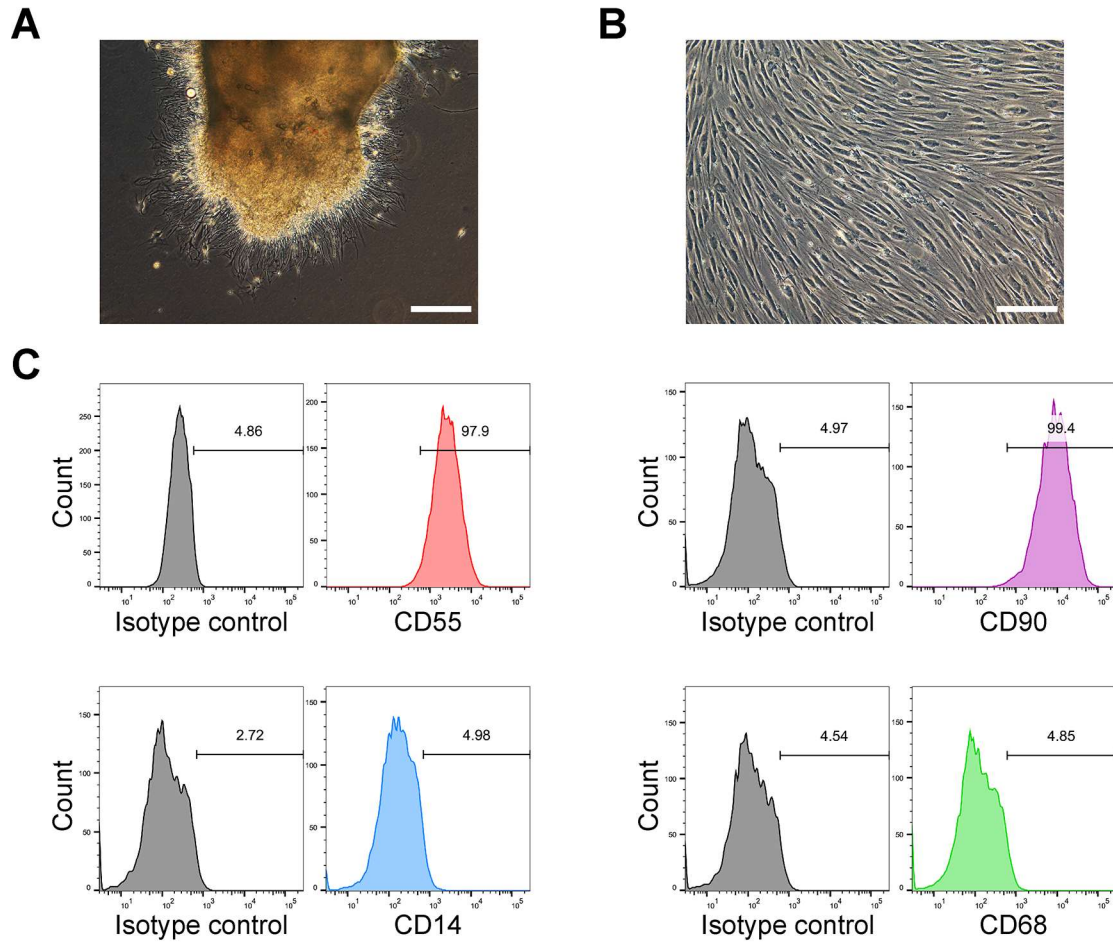


Figure S1. The morphological characters and surface molecules expression of RA-FLSs.

(A) The primary cell crawled out from synovial tissues within seven days. Scale bar, 200 μm. **(B)** RA-FLSs at passage three were characterised as spindle cell morphology and woven shape under an optical microscope. Scale bar, 200 μm. **(C)** The surface molecules of RA-FLSs at passage three were characterised by flow cytometry. Isotype-matched antibodies were used as methodologic controls, respectively. The high rate of CD55 and CD90, and the negative staining of CD14 and CD68, indicate the high purity of RA-FLSs used in the study.

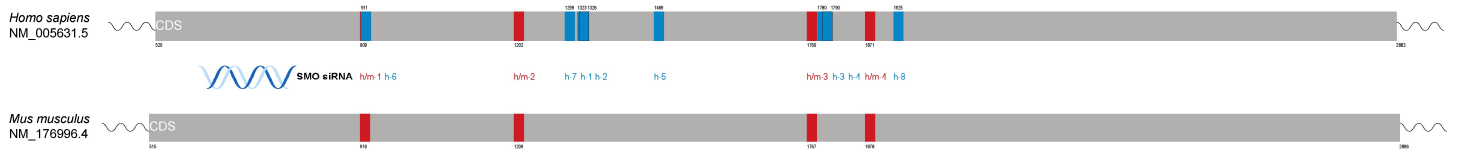


Figure S2. The target sites of anti-SMO siRNAs.

The target sites of anti-SMO siRNAs against the SMO mRNA coding sequences in *Homo sapiens* (blue) and *Mus musculus* (red).

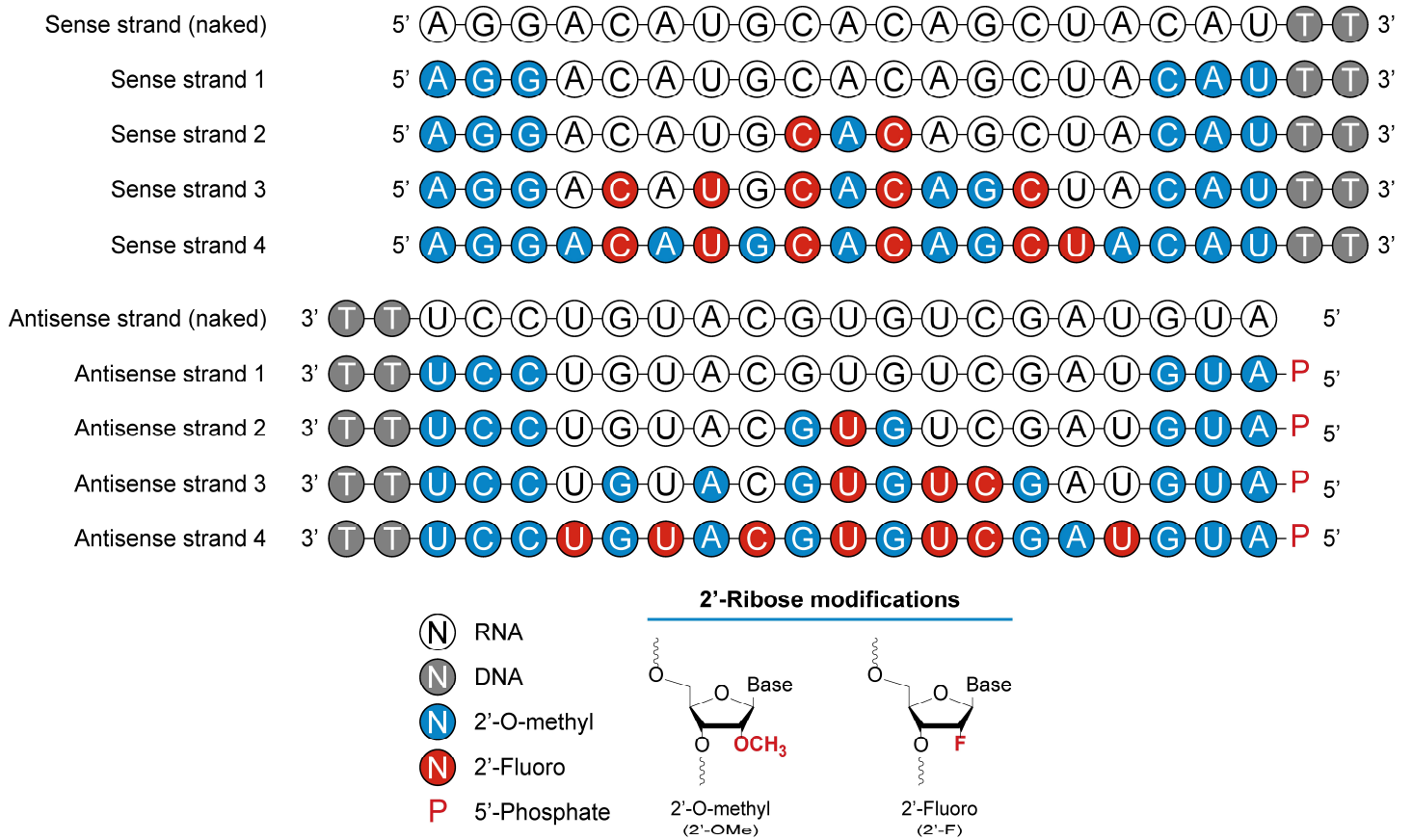


Figure S3. Chemical modifications patterns of si-h/m-2.

Chemical modifications including 2'-O-methyl, 2'-fluoro, and 5'-phosphate were introduced to different sites of the sense strand (called sense strand 1 to 4) and antisense strand (called antisense strand 1 to 4) of si-h/m-2. Schematic diagrams of naked siRNA and chemically modified siRNAs were shown.

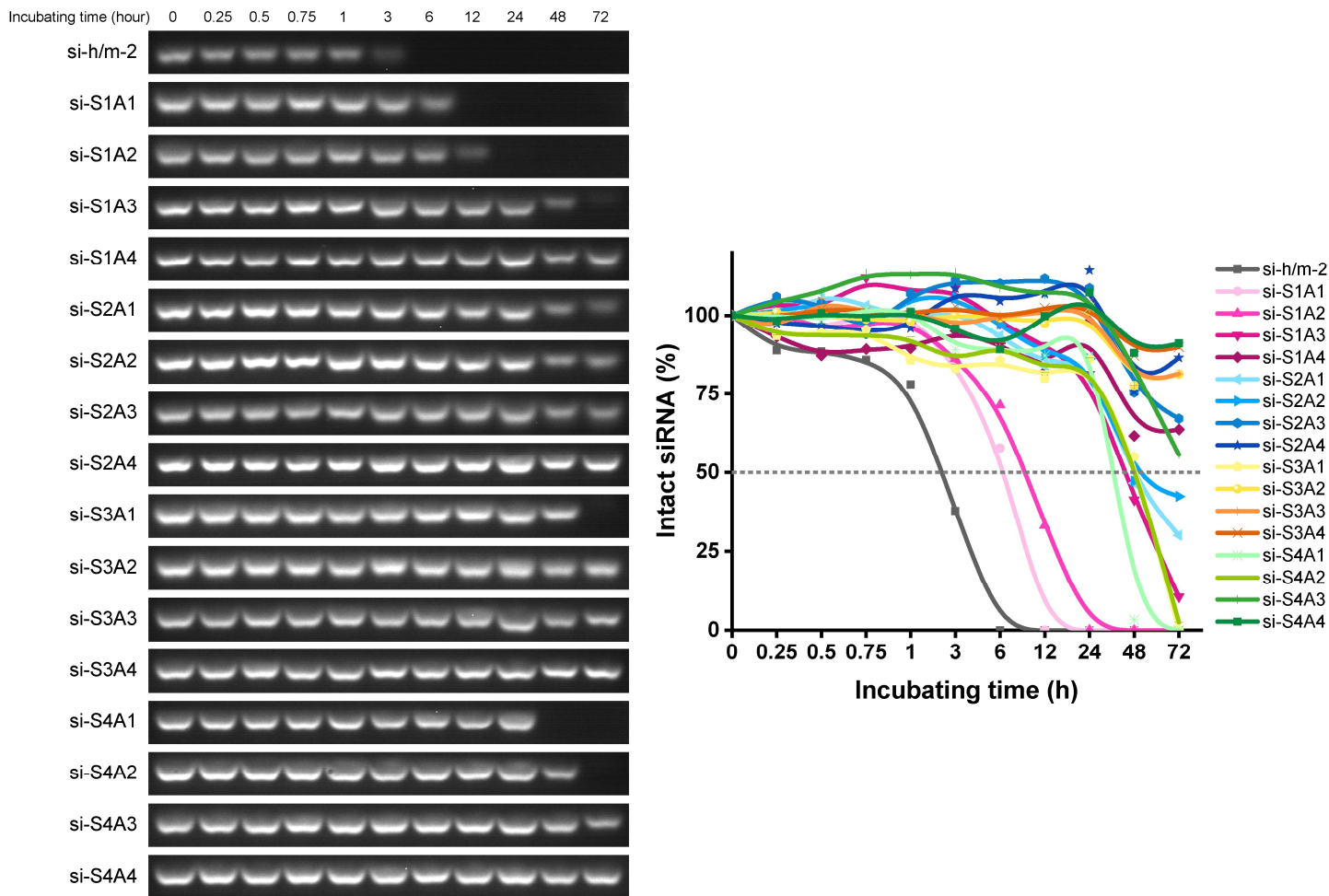


Figure S4. Chemical modifications enhance the stabilities of siRNA.

The agarose gel electrophoresis showed the stability of chemically modified siRNA incubated in human serum for the indicated time. The si-h/m-2 (naked siRNA) was used as a control. The percentages of intact siRNA after incubating for the indicated time were shown in the line chart (n = 1).

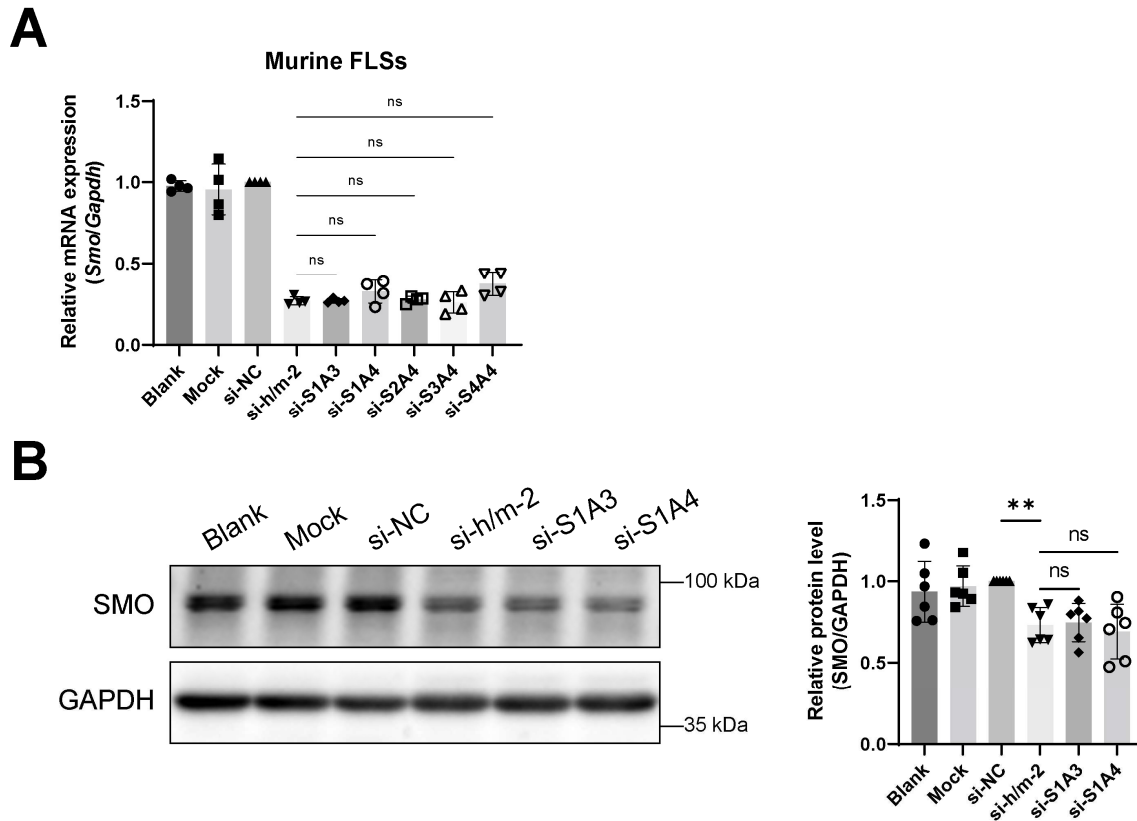


Figure S5. Chemically modified siRNAs inhibit SMO expression with high efficiency in murine FLSs.

(A) Comparison of silencing efficiency between naked siRNA and chemically modified siRNAs. Relative Smo mRNA expression was quantified by qPCR after murine FLSs were transfected with naked siRNA or chemically modified siRNAs (50 nM) for 48 h and shown as fold change versus si-NC (50 nM) ($n = 4$). **(B)** Representative western blot of SMO protein after murine FLSs were transfected with si-h/m-2, si-S1A3, or si-S1A4 (50 nM) for 72 h. GAPDH was used as a loading control. Relative expression was calculated as the ratio of SMO/GAPDH and presented as fold change versus si-NC (50 nM) ($n = 6$). Statistics: Data were presented as mean \pm SD; ns $P > 0.05$, $**P < 0.01$ versus si-NC group by one-way ANOVA with Dunnett's test for multiple comparisons.

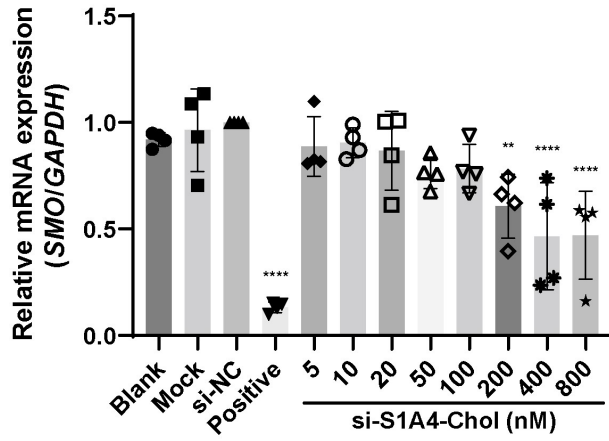


Figure S6. Cholesterol-conjugated chemically modified siRNAs inhibit SMO mRNA expression without the transfection reagent.

Concentration dependence of si-S1A4-Chol in the silence of SMO mRNA expression was determined by qPCR after RA-FLSs were transfected with si-S1A4-Chol at indicated concentrations without any transfection reagent for 48 h, si-S1A4 (50 nM) transfected with transfection reagent was served as the positive control, and relative expression was shown as fold change versus si-NC (50 nM) ($n = 4$). Statistics: Data were presented as mean \pm SD; ** $P < 0.01$, **** $P < 0.0001$ versus si-NC group by one-way ANOVA with Dunnett's test for multiple comparisons.

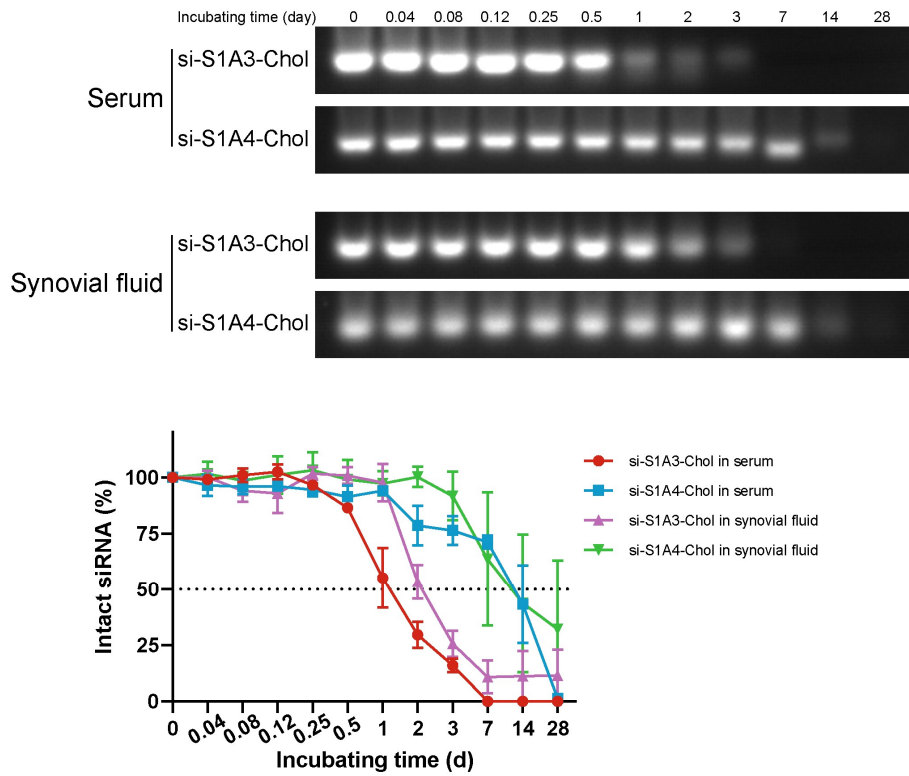


Figure S7. Chemical modifications enhance the stabilities of siRNA in synovial fluids.

The representative agarose gel electrophoresis showed the stability of cholesterol-conjugated chemically modified siRNAs incubated in human serum and rheumatoid arthritis synovial fluids for the indicated time. The percentages of intact siRNA after incubating for the indicated time were shown in the line chart (n = 3).

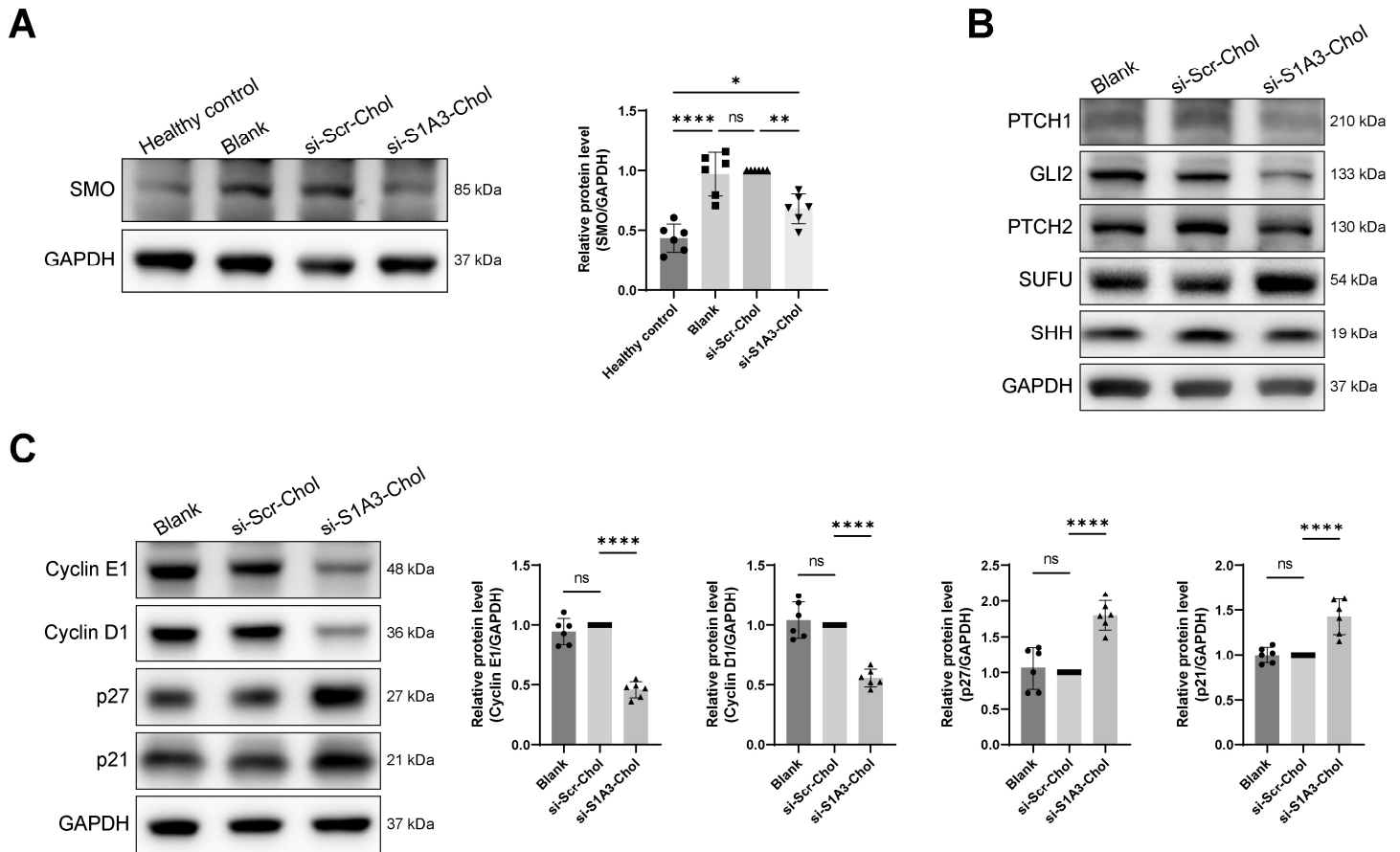


Figure S8. Chemically modified siRNAs inhibit the activity of Hedgehog signalling pathway in RA-FLSs.

(A) The SMO protein level was over-expressed in RA-FLSs compared with FLSs from healthy control, and was reduced in RA-FLSs treating with si-S1A3-Chol (800 nM) for 72 h. GAPDH was used as a loading control. Relative expression was calculated as the ratio of protein/GAPDH and presented as fold change versus si-Scr-Chol (n = 6). **(B)** The inhibiting effect on hedgehog signalling pathway after si-S1A3-Chol treatment. Representative western blot of proteins in total protein after RA-FLSs were treated with si-Scr-Chol or si-S1A3-Chol (800 nM) for 72 h. GAPDH was used as a loading control. **(C)** The inhibiting effect on cell cycle pathway after si-S1A3-Chol treatment. Representative western blot of proteins in total protein after RA-FLSs were treated with si-Scr-Chol or si-S1A3-Chol (800 nM) for 72 h. GAPDH was used as a loading control. Relative expression was calculated as the ratio of protein/GAPDH and presented as fold change versus si-Scr-Chol (n = 6).

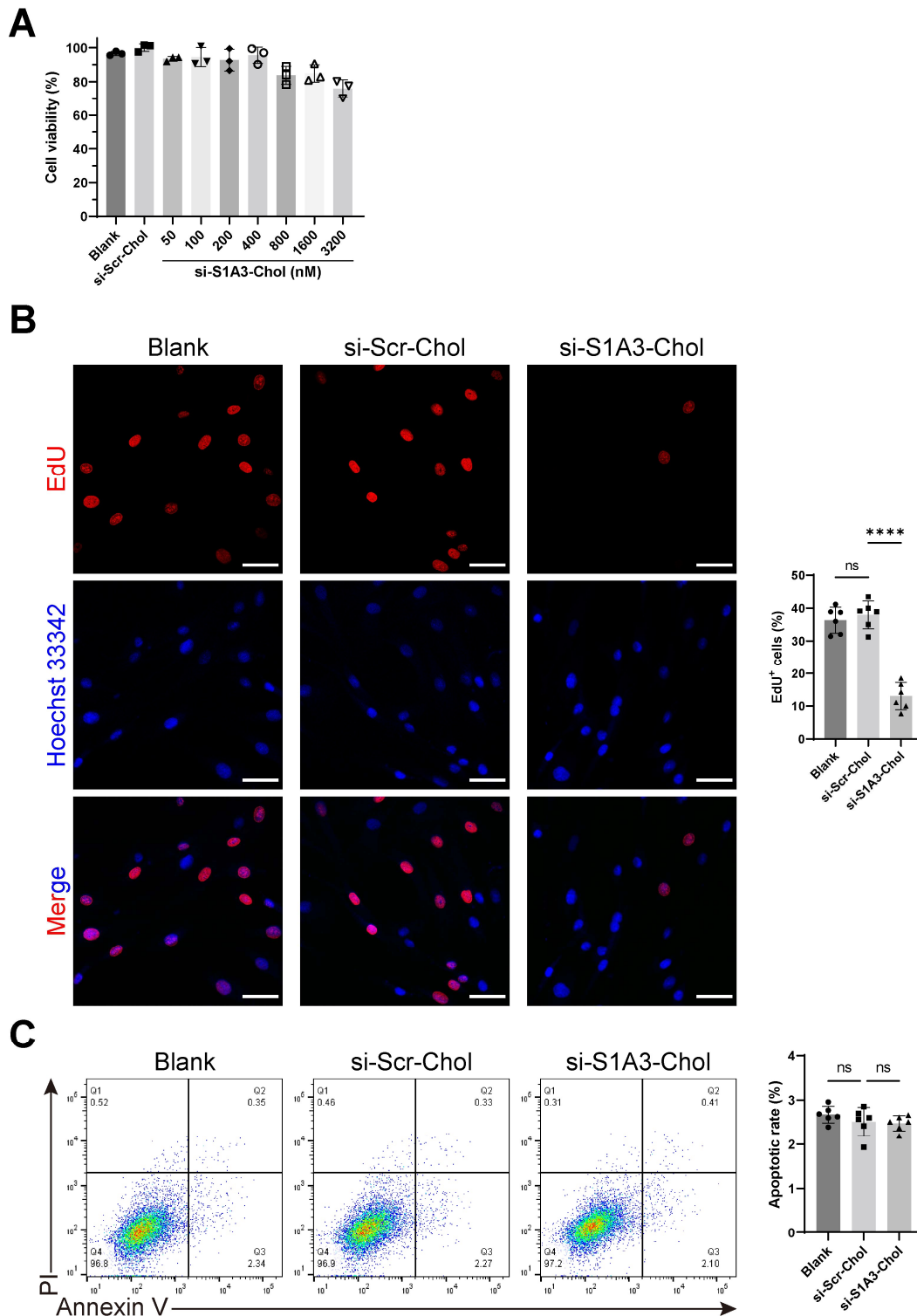


Figure S9. Cholesterol-conjugated chemically modified siRNA affects RA-FLSs cell proliferation.

(A) The impact on cell viability was evaluated by CCK-8 assay after RA-FLSs treated with si-Scr-Chol (800 nM) or si-S1A3-Chol at indicated concentration for 48 h, and shown as percentages of si-Scr-Chol (n= 3). (B) The effect of si-S1A3-Chol on cell proliferation was determined by EdU assay. Proliferative RA-FLSs were stained with EdU (red signal). Cell nuclei are stained with Hoechst 33342 (blue signal). The percentages of EdU positive cells were detected by confocal microscope after RA-FLSs treated with si-Scr-Chol or si-S1A3-Chol (800 nM) for 48 h and shown in the bar graph (n = 6). Scale bar, 50 μ m. (C) The effect of si-S1A3-Chol on cell apoptosis was determined by Annexin V/PI assay. The percentages of Annexin V positive cells were detected by flow cytometry after RA-FLSs treated with si-Scr-Chol or si-S1A3-Chol (800 nM) for 48 h and shown in the bar graph (n = 6). Statistics: Data were presented as mean \pm SD; ns $P > 0.05$, **** $P < 0.0001$ versus si-Scr-Chol group by one-way ANOVA with Dunnett's test for multiple comparisons.

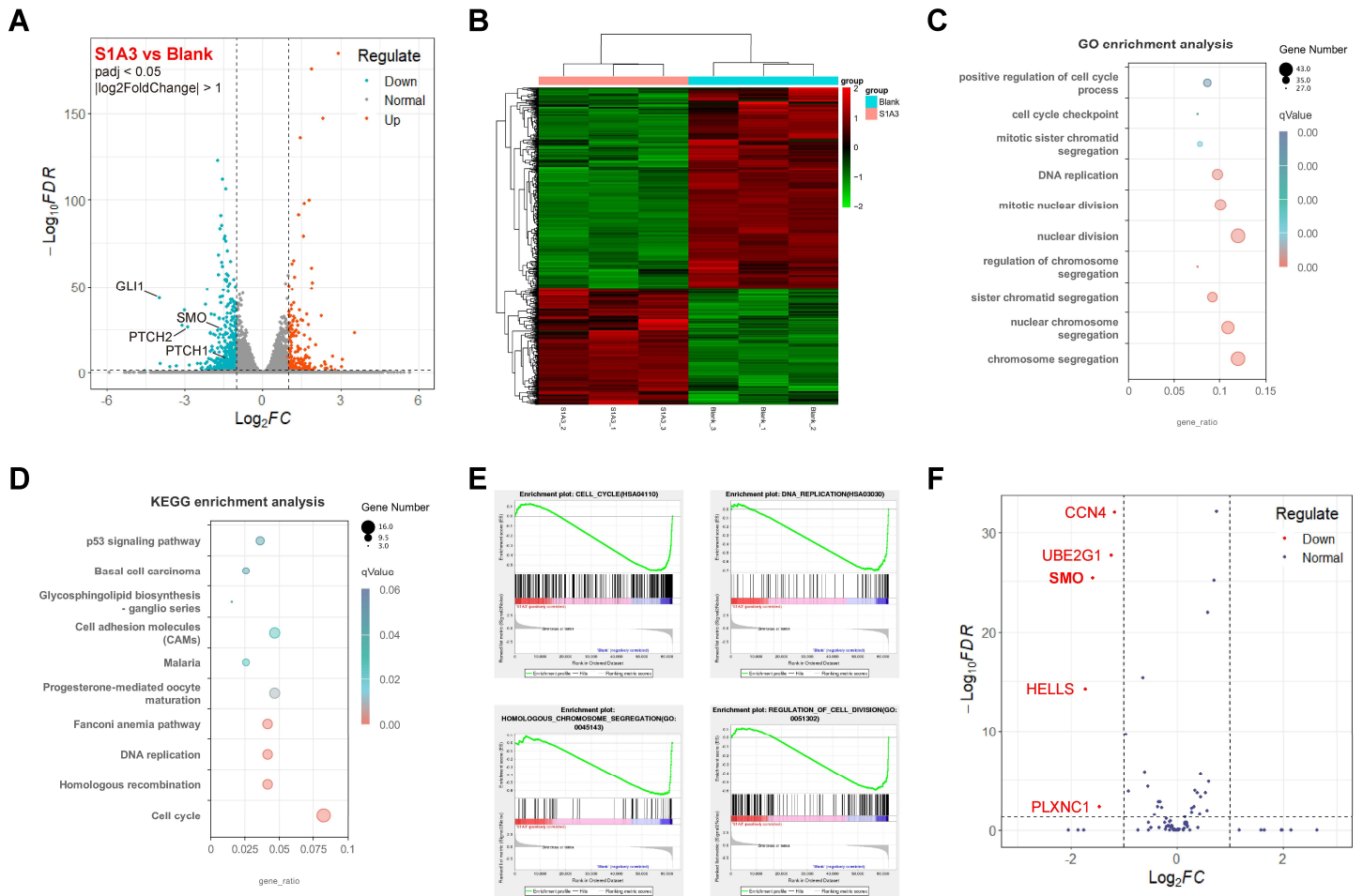


Figure S10. RNA-seq reveals the mechanisms and off-target effects of si-S1A3-Chol on RA-FLSs.

(A) Volcano plot and (B) heatmap plot revealed the differential genes expression after RA-FLSs treated with si-S1A3-Chol (800 nM) for 48 h. Genes with an adjusted *P*-value less than 0.05 and absolute fold change of 2 were considered as differentially expressed. (C) GO enrichment analysis, (D) KEGG pathway enrichment analysis, and (E) gene set enrichment analysis were performed to determine the differential genes enrichment and clarify the regulation mechanism of si-S1A3-Chol treatment in RA-FLSs. (F) Volcano plot showed the expression of top 100 similar transcripts in RA-FLSs treating with si-S1A3-Chol (800 nM) for 48 h. The down-regulated genes were label in red.

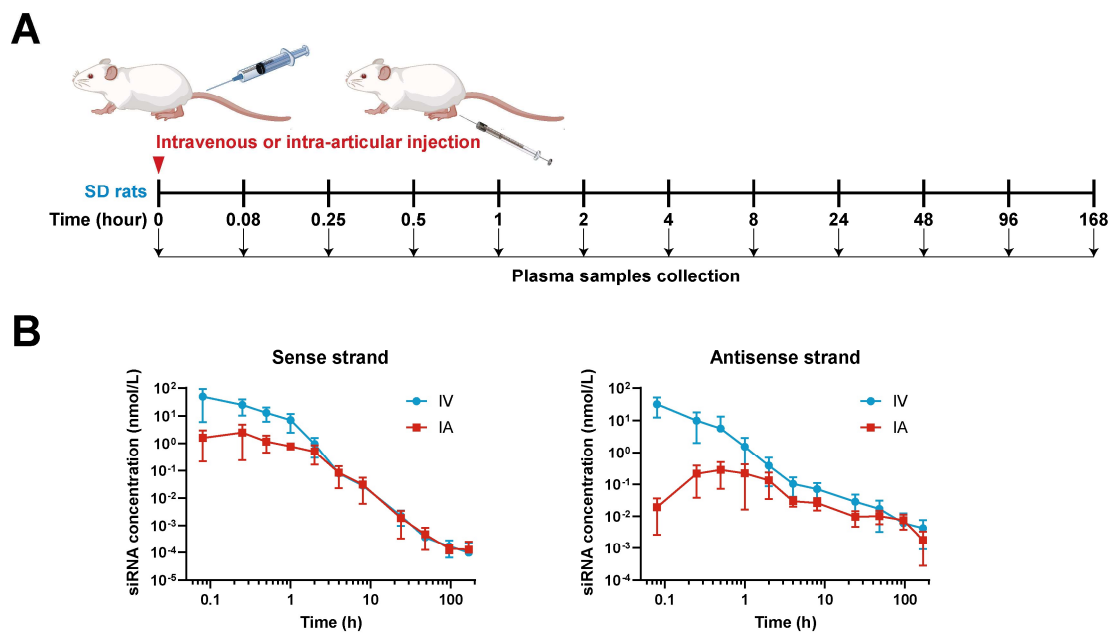


Figure S11. Intra-articular injection reduces the amount of si-S1A3-Chol in blood circulation.

(A) The schematic diagram of siRNA pharmacokinetics studies in SD rats. SD rats were injected with single dose si-S1A3-Chol (25 nmol/kg dose of body weight) intravenously or intra-articularly, and the plasma samples were collected at indicated time points. (B) The concentration of sense strand (left) and antisense strand (right) of siRNA in plasma from rats with the si-S1A3-Chol administrated by intravenous injection or intra-articular injection (n = 3).

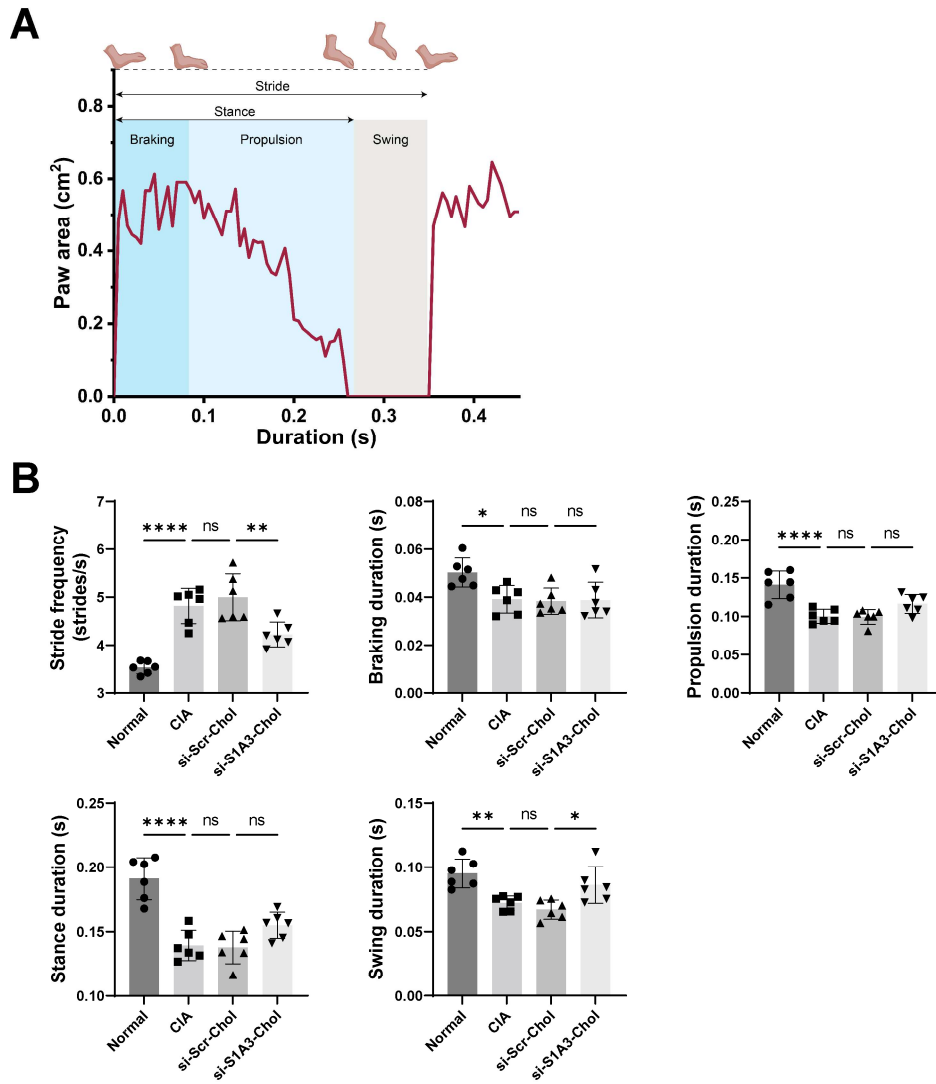


Figure S12. Cholesterol-conjugated chemically modified siRNA alleviates the gait dysfunction in CIA mice.

(A) The schematic diagram of a complete stride phase in gait analysis. A full stride comprised braking, propulsion, stance and swing phases. **(B)** The effect of si-S1A3-Chol on stride frequency, braking duration, propulsion duration, stance duration, and swing duration of CIA mice were measured in gait analysis ($n = 6$). Statistics: Data were presented as mean \pm SD; ns $P > 0.05$, $*P < 0.05$, $**P < 0.01$, $****P < 0.0001$ versus between groups by one-way ANOVA with Dunnett's test for multiple comparisons.

Movie S1. Cholesterol-conjugated chemically modified siRNA reverses the gait dysfunction in CIA mice.

The motor function of CIA mice was assessed by gait analysis. Representative ventral images were captured, and the digital footprints were generated. The paw area and stride frequency were increased in CIA mice. si-S1A3-Chol reduced the paw area and stride frequency, showing the effect on reversing gait dysfunction.